Proceedings of the 2002 IEEE
International Symposium on Intelligent Control
Vancouver, Canada • October 27-30, 2002

Stereo Vision Guided Control of a Stewart Platform

Aiqiu Zuo and Q.M. Jonathan Wu

Vision and Sensing Group

Innovation Center
National Research Council Canada
Vancouver, BC V6T 1W5 Canada

William A. Gruver

Intelligent Robotics & Manufacturing Systems Laboratory
School of Engineering Science
Simon Fraser University
Burnaby, BC V5A 1S6 Canada

Abstract

This paper presents a new implementation of closed-loop pose control for a Stewart platform. We use stereo vision to measure the pose of the Stewart platform in real time. Because only three feature points are necessary for pose measurement, the computational requirements for image processing and calculation are small. The measured pose provides feedback to the inverse kinematics of the Stewart platform so that the pose error can be compensated. Experimental results are provided to show the ability of the method to control the pose.

1. Introduction

A Stewart platform is a six degree of freedom mechanism consisting of a movable platform, fixed base, 12 spherical joints, and 6 links whose length is adjustable using prismatic actuators, as shown in Fig. 1. The pose of the Stewart platform is the position and orientation of the movable platform relative to a world coordinate system.

The Stewart platform is superior to serial manipulators because of its high stiffness, high load-carrying capacity, and high dynamic performance. Many applications involving robotic manipulation require an accurate pose.

Typically, the control of a Stewart platform utilizes software based on the inverse kinematics. However, factors such as manufacturing tolerances, installation errors, and link offsets cause deviations to the nominal kinematic parameters, thereby resulting in an inaccurate pose. Methods that have been used to measure the pose of serial manipulators are not suitable, particularly in mechanisms having limited actuator accessibility and large structures.

To improve the pose accuracy of a Stewart platform, Wang and Masory [1] developed a kinematic model to accommodate deviations of nominal kinematic parameters and evaluated the effect of these parameters on the pose accuracy. Behi [2] developed modified algorithms for the forward and inverse kinematics. Calibration methods have been presented to determine the actual values of the link lengths [3][4-7]. Wu [8] controlled a Stewart platform with the pose computed by the forward kinematics based on the measurement of the link lengths. In all the latter systems, the Stewart platform was subject to open-loop control.

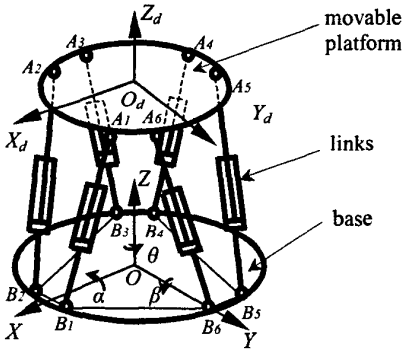

Fig.1 Stewart platform

This paper describes a new approach for closed-loop pose control of a Stewart platform. By using stereo visual information, 3D positions of three feature points on the movable platform are obtained in order to determine the pose of the Stewart platform. The measured pose provides feedback to the inverse kinematics of the Stewart platform so that the pose error can be reduced.

2. Inverse Kinematics

The inverse kinematic solution of the Stewart platform provides a means to obtain the link lengths as a function of the position, *(x, y, z)*, and orientation, (α , β , θ), referenced to a world coordinate system [8].

2.1. Vector Relationships

We define the world coordinate system XYZ and the dynamic coordinate system $X_dY_dZ_d$ as illustrated in Fig.1. When the movable platform moves within its workspace, the dynamic motion is relative to an intermediate coordinate system $X_{dm}Y_{dm}Z_{dm}$. It is assumed that translation only occurs along the Z-axis between XYZ and $X_{dm}Y_{dm}Z_{dm}$.

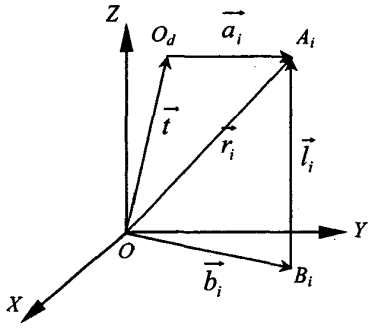

Fig. 2 Vector relationships

Then, as shown in Fig. 2,

$$\vec{r}_i = \vec{a}_i + \vec{t} \tag{1}$$

$$\vec{r}_i = \vec{b}_i + \vec{l}_i \tag{2}$$

from which we obtain

$$\vec{l}_i = \vec{a}_i + \vec{t} - \vec{b}_i \tag{3}$$

where $\vec{r}_i$ is the position vector of the joint A_i; $\vec{a}_i$ is the position vector of the joint A_i in the dynamic coordinate system; $\vec{b}_i$ is the position vector of the joint B_i; $\vec{l}_i$ is the length of the ith link; $\vec{t}$ is the translation of the movable platform; and $i=1,...,6$. In all cases the vectors are referenced to the world coordinates.

2.2. Inverse Kinematic Solution

In Eq. (3) $\vec{b}_i$ is a constant vector. For a given pose $(x, y, z, \alpha, \beta, \theta)$, we have $\vec{t} = [x, y, z]'$. Suppose

$$n' = R\ n'_d \tag{4}$$

where n' is a unit vector referenced to the dynamic coordinate system; n'_d is a unit vector referenced to the world coordinate system; and R is the rotation transformation matrix;

$$R = \begin{bmatrix} \cos\theta\cdot\cos\beta & \cos\theta\cdot\sin\beta\cdot\sin\alpha - \sin\theta\cdot\cos\alpha & \sin\theta\cdot\sin\alpha + \cos\theta\cdot\sin\beta\cdot\cos\alpha \\ \sin\theta\cdot\cos\beta & \cos\theta\cdot\cos\alpha + \sin\theta\cdot\sin\beta\cdot\sin\alpha & \sin\theta\cdot\sin\beta\cdot\cos\alpha - \cos\theta\cdot\sin\alpha \\ -\sin\beta & \cos\beta\cdot\sin\alpha & \cos\beta\cdot\cos\alpha \end{bmatrix} \tag{5}$$

Then

$$\vec{a}_i = R\ \vec{a}_i^{\,d} \tag{6}$$

where $\vec{a}_i^{\,d}$ is the position vector of the joint A_i referenced to the dynamic coordinate system. Combing Eq. (3) and Eq. (6), we obtain

$$\vec{l}_i = R\ \vec{a}_i^{\,d} + \vec{t} - \vec{b}_i \tag{7}$$

The change of the link length is

$$s_i = \left|\vec{l}_i\right| - \left|\vec{l}_i^{\,m}\right| \tag{8}$$

where $\left|\vec{l}_i^{\,m}\right|$ is the ith link length for the known intermediate position.

2.3. Link Control

Fig.3 illustrates a control system based on the inverse kinematic solution. Microcontrollers are used to process joint commands from the host computer. Although each link has closed-loop control, the overall system is open loop and may not adequately compensate errors that result from manufacturing tolerances, installation errors, and link offsets.

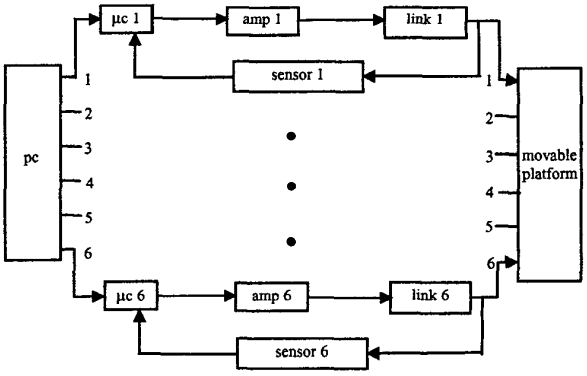

Fig. 3 Link control system

3. Pose Measurement by Stereo Vision

We employ a stereo vision system consisting of two fixed CCD cameras to view the movable platform as shown in Fig. 4. By this means, the image coordinates of feature points can be obtained, the 3D positions of feature

points can be reconstructed and an accurate pose of the Stewart platform can be obtained.

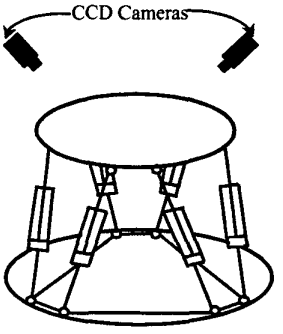

Fig. 4 Stewart platform with stereo cameras

3.1. Feature Points

As shown in Fig.5, three circular shapes are placed on the movable platform and their centers P_1, P_2 and P_3 serve as feature points. We also invoke the following assumptions.

- Feature points have high contrast
- Feature points do not lie on a straight line
- Feature points are visible throughout the entire workspace;
- The motion of the Stewart platform is slow compared with the time needed for image acquisition and processing.

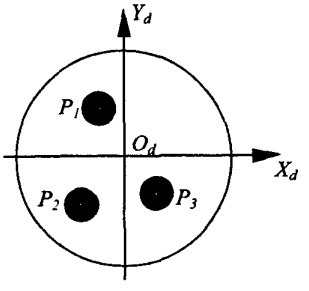

Fig. 5 Location of feature points

Assumption 1 is needed for rapid image processing. Assumption 2 ensures that the feature points possess enough information to determine the pose of the Stewart platform. Assumption 3 ensures that any pose of the Stewart platform within its workspace can be measured. Finally, Assumption 4 ensures that the stereo images are not blurred.

For real-time operation, it is critically important to select efficient methods that avoid time-consuming computation. Our approach consists of two steps, compute initial image coordinates of the feature points when the platform is stationary and then dynamically track them during platform motion. Stereo matching of feature points is determined from the relative positions of the feature points.

3.2. Mapping from Image Coordinates to 3D Coordinates

The image coordinates of feature point j under stereo projection are given by

$$\overrightarrow{p^I_{j,1}} = P_1\ C_1\ S_1\ \overrightarrow{p_j} = K_1\ \overrightarrow{p_j} \tag{9}$$

$$\overrightarrow{p^I_{j,2}} = P_2\ C_2\ S_2\ \overrightarrow{p_j} = K_2\ \overrightarrow{p_j} \tag{10}$$

where S_i is the rotation transformation matrix of the i th camera coordinate system relative to the intermediate coordinate system; C_i is the translation transformation matrix of the i th camera coordinate system relative to the intermediate coordinate system; P_i is the perspective matrix of the i th camera; K_i is a mapping matrix from 3D coordinates (with respect to the intermediate coordinate system) to image coordinates of the i th camera; $\overrightarrow{p_j}$ are the 3D coordinates of the j th feature point referenced to the intermediate coordinate system; $\overrightarrow{p^I_{j,i}}$ are the image coordinates of the j th feature point with the i th camera; and $i=1,2, j=1,2,3$.

To reconstruct the 3D coordinates of feature points, stereo calibration is needed. This results in

$$\overrightarrow{p^I_{j,i}} = g(\overrightarrow{p_j}) \tag{11}$$

which can be rewritten as

$$\overrightarrow{p_j} = h(\overrightarrow{p^I_{j,i}}) \tag{12}$$

where $g(\ )$ is a mapping from 3D coordinates (referenced to the intermediate coordinate system) to image coordinates, and $h(\ )$ is a mapping from image coordinates to 3D coordinates referenced to the intermediate coordinate system.

From Eq. (12), the 3D feature points referenced to the intermediate coordinate system $\overrightarrow{p_j}$ can be reconstructed.

3.3. Pose Determination

When the movable platform moves within its workspace, as shown in Fig. 6, the Cartesian coordinates of the jth feature point can be expressed as

$$\overrightarrow{p_j} = \overrightarrow{p_j^m} + \vec{t'} \tag{13}$$

where $\overrightarrow{p_j^m}$ is the position vector of the jth feature point in the dynamic coordinate system referenced to the intermediate coordinate system, $\overrightarrow{p_j^m} = [x_j^m \quad y_j^m \quad z_j^m]'$, $j=1,2,3$; and $\vec{t'}$ is a translation vector of the movable platform referenced to the intermediate coordinate system.

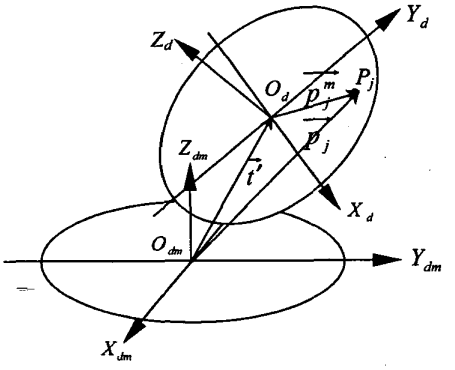

Fig. 6 Movable platform

We also have

$$\overrightarrow{p_j^m} = R\ \overrightarrow{p_j^d} \tag{14}$$

where $\overrightarrow{p_j^d}$ is the position vector of the j th feature point referenced to the dynamic coordinate system, $\overrightarrow{p_j^d} = [x_j^d \quad y_j^d \quad z_j^d]'$, for $j=1,...,3$;

We combine Eqs. (13) and (14),

$$\overrightarrow{p_j} = R\ \overrightarrow{p_j^d} + \vec{t'} \tag{15}$$

where $\overrightarrow{p_j^d}$ is known and $\overrightarrow{p_j}$ can be obtained from Eq. (12). Suppose there are two feature points, P_1 and P_2. Then, we obtain

$$\overrightarrow{p_1} = R\ \overrightarrow{p_1^d} + \vec{t'} \tag{16}$$

$$\overrightarrow{p_2} = R\ \overrightarrow{p_2^d} + \vec{t'} \tag{17}$$

Subtracting Eq. (17) from Eq. (16),

$$\overrightarrow{p_1} - \overrightarrow{p_2} = R\ (\overrightarrow{p_1^d} - \overrightarrow{p_2^d}) \tag{18}$$

From Eq. (18) we obtain three equations with three unknowns (α, β, θ) that can be computed. However, because Eq. (18) is set of nonlinear equations, it may be difficult to solve accurately.

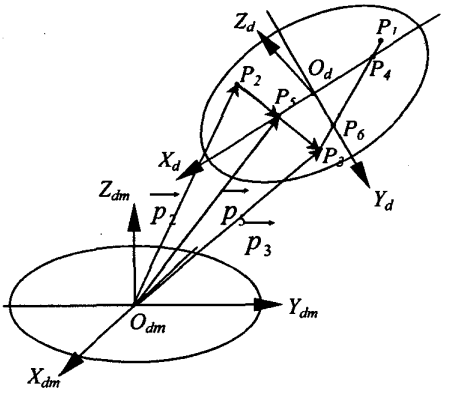

Fig. 7 Platform Geometry

As shown in Fig. 7, P_2P_3 crosses X_d at P_5 and P_1P_3 crosses X_d and Y_d at P_4 and P_6, respectively. From the feature points we obtain P_4, P_5 and P_6, and

$$\overrightarrow{p_5^d} = [x_5^d \quad 0 \quad 0]' \tag{19}$$

$$\overrightarrow{p_6^d} = [0 \quad y_6^d \quad 0]' \tag{20}$$

By defining

$$\lambda_5 = \frac{\left|\overrightarrow{p_{25}}\right|}{\left|\overrightarrow{p_{53}}\right|} = \frac{|p_2p_5|}{|p_5p_3|} \tag{21}$$

$\overrightarrow{p_{25}}$ can be expressed as

$$\overrightarrow{p_{25}} = \overrightarrow{p_{23}} \frac{\lambda_5}{1+\lambda_5} \tag{22}$$

The Cartesian coordinates of P_5 are

$$\overrightarrow{p_5} = \overrightarrow{p_2} + \overrightarrow{p_{25}} \tag{23}$$

and $\overrightarrow{p_4}$, $\overrightarrow{p_6}$ can also be obtained in a similar manner. From $\overrightarrow{p_4}$ and $\overrightarrow{p_5}$, the position of O_d, the position of the Stewart platform referenced to the intermediate coordinate system $\vec{t'}$, can be obtained. Then from Eq. (12) and Eq. (13), $\overrightarrow{p_5^m}$ can be computed. Combining Eq. (5), Eq. (14), and Eq. (19), we have

$$\begin{bmatrix} x_5^m \\ y_5^m \\ z_5^m \end{bmatrix} = \begin{bmatrix} \cos\theta \cdot \cos\beta \cdot x_5^d \\ \sin\theta \cdot \cos\beta \cdot x_5^d \\ -\sin\beta \cdot x_5^d \end{bmatrix} \tag{24}$$

from which we obtain

$$\beta = \arcsin(-z_5^m / x_5^d)$$

$$\theta = \arcsin(y_5^m / (x_5^d \cdot \cos\beta))$$

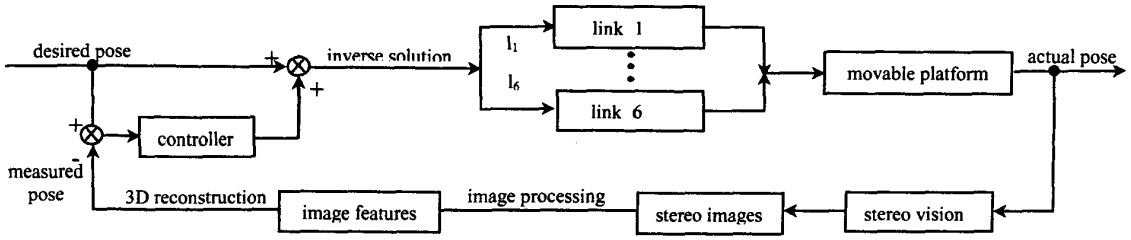

Fig. 8 Vision guided control system

Similarly, we have

$$\begin{bmatrix} x_6^m \\ y_6^m \\ z_6^m \end{bmatrix} = \begin{bmatrix} (\cos\theta \cdot \sin\beta \cdot \sin\alpha - \sin\theta \cdot \cos\alpha) \cdot y_6^d \\ (\cos\theta \cdot \cos\alpha + \sin\theta \cdot \sin\beta \cdot \sin\alpha) \cdot y_6^d \\ \cos\beta \cdot \sin\alpha \cdot y_6^d \end{bmatrix} \quad (25)$$

Then α can be computed by

$$\alpha = \arcsin(\, z_6^m / (\cos\, \beta \cdot y_6^d))$$

For feature point P_1, Eq. (15) can also be written as

$$\vec{t'} = \overrightarrow{p_1} - R\ \overrightarrow{p_1^d} \quad (26)$$

Substituting the computed rotation angle into Eq. (26), we obtain $\vec{t'}$. Then the translation vector $\vec{t}$ is

$$\vec{t} = \vec{t'} + \vec{t_m} \quad (27)$$

where $\vec{t_m}$ is the translation vector of the intermediate coordinate system relative to world coordinate system.

4. Experimental Results

An experimental system has been built in which the Stewart platform was controlled by electro-hydraulic actuators. The radii of the movable platform and the base were 0.6 m and 0.8 m, respectively. The pose of the Stewart platform was detected by stereo vision to provide feedback to the control system for comparison with the desired pose. By inverse kinematics, we obtained the changes in link lengths needed to drive the pose error to zero. The closed loop response of the Stewart platform was approximately 1 Hz. CCD cameras with a. resolution of 768 x 576 were employed in the stereo vision system. The radius of each of feature point was 100 mm. Approximately 80 ms was required for image acquisition and processing of the stereo images and calculating the final pose. The closed-loop vision-guided control system is shown in Fig. 8.

Our experiments achieved 6-axis closed loop control of the movable platform at uniform velocities within 20 seconds. The limits of motion were: x = 150 *mm*; y = 150 *mm*; z = 50 *mm*; α = 5°; β: 5°; and θ = 10°. The experimental results are shown in Figs. 9(a) and 9(b), respectively. Table 1 indicates the pose accuracy of the vision guided control system. In our experiments, the average pose accuracy was 35.8%. The translation accuracy was 29.4% and the rotation accuracy was 42.1%.

Table 1 compares $e^{a,o}$, the pose error under open-loop control for a=x, y,z,α,β,θ; $e^{a,c}$, the pose error under closed-loop control for a= x,y,z,α,β,θ; δ^a, the percent improvement of the pose accuracy under closed-loop control for a= x,y,z,α,β,θ; δ^t is the average percent improvement of the translation accuracy under closed-loop control; δ^r is the average percent improvement of the rotation accuracy under closed-loop control; δ^{3t}, the percent improvement of the 3D translation accuracy under closed-loop control; and δ, the average percent improvement of six degrees of freedom under closed-loop control. Translation was measured in millimeters and rotation was measure in radians.

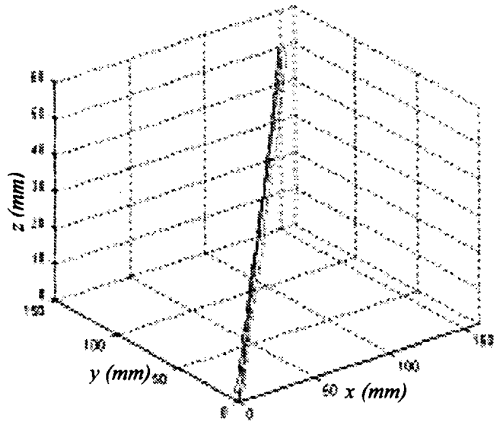

Fig. 9 Comparison of measured pose (a) 3D translation

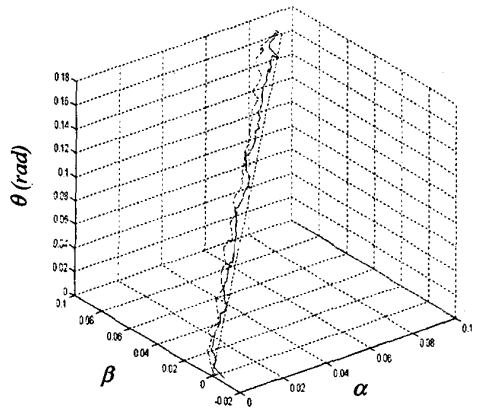

Fig. 9 Comparison of measured pose (b) 3D rotation

	$e^{a,o}$	$e^{a,c}$	δ^a	δ^t (δ^r)	δ^{3t}	δ
x	3.00444	2.09588	0.30241			
y	0.88202	0.61825	0.29905	0.29393	0.29974	
z	1.09267	0.78637	0.28032			
α	0.00138	8.99412e-4	0.34825			0.35722
β	0.00552	0.00261	0.48111	0.42051		
θ	0.00503	0.00586	0.43217			

Table 1 Pose Accuracy

5. Conclusions

We described an approach for closed-loop pose control of a Stewart platform. Stereo vision was employed to measure the pose of the Stewart platform in real time and provide feedback to the links to reduce the pose error.

Experimental results demonstrate the effectiveness of the method to improve the pose accuracy of the Stewart platform. The computational requirements are not excessive because it is not necessary to solve the forward kinematics, a difficult task for parallel manipulators. Finally, the method provides improvement of the pose accuracy of the Stewart platform over its workspace.

References

[1] J. Wang and O. Masory. "On the Accuracy of a Stewart Platform - Part1: The Effect of Manufacturing Tolerances," *Proceedings of the 1993 IEEE International Conference on Robotics and Automation*, 1993, pp 114-120.

[2] F. Behi. "Kinematic Analysis for a Six-Degree-of Freedom 3-PRPS Parallel Mechanism," *IEEE Journal of Robotics and Automation*, Vol. 4, No. 5, October 1988, pp 561-565.

[3] H. Zhang, O. Masory, and J. Yan. "Kinematic Calibration of a Stewart Platform using Pose Measurements Obtained by a Single Theodolite," *Proceedings of the 1995 IEEE/RSJ International Conference on Intelligent Robots and Systems*, Vol. 2, 1995, pp 329-334.

[4] W. Khalil and S. Besnard. "Self-Calibration of Stewart-Gough Parallel Robots without Extra Sensors," *IEEE Transactions on Robotics and Automation*, Vol. 15, No. 6, pp 1116-1121.

[5] A. Nahvi, J. Hollerbach, and V. Hayward. "Calibration of a Parallel Robot using Multiple Kinematic Closed Loops," *Proceedings of the 1994 IEEE International Conference on Robotics and Automation*, May 1994, pp 407-412.

[6] H. Zhang. "Self-Calibration of Parallel Mechanisms with a Case Study on Stewart Platforms," *IEEE Transactions on Robotics and Automation*, Vol. 13, No. 3, June 1997, pp 387-397.

[7] O. Masory, J. Wang, and H. Zhuang. "On the Accuracy of a Stewart Platform-Part 1: Kinematic Calibration and Compensation," *Proceedings of the 1993 IEEE International Conference on Robotics and Automation,* May 1993, pp 725-731.

[8] J. Wu. *Study of a Parallel 6 Degree of Freedom Platform and its Control*, Ph.D. Thesis, Zhejiang University, China, 1996.